Advances in Science and Technology Research Journal

*Advances in Science and Technology Research Journal*, 2025, 19(6), 342–352
https://doi.org/10.12913/22998624/203267
ISSN 2299-8624, License CC-BY 4.0

Received: 2025.03.11
Accepted: 2025.04.15
Published: 2025.05.01

# Buckling behaviour of cold-formed steel channel section, sigma section, and built-up sigma section: Experimental and numerical study

Vaishnavi Prabaharan[1], Punitha Kumar Akhas[1*]

[1] Vellore Institute of Technology, School of Civil Engineering, Vellore, Tamil Nadu 632014, India
* Corresponding author's e-mail: punithakumar.a@vit.ac.in

## ABSTRACT

In the construction industry, cold-formed steel sections (CFS) are highly preferred in purlins, girts, studs in walls, and shear wall chords. Based on its strength requirements, CFS can be produced in the desired cross-sectional dimensions and shapes. The majority of wall studs are made of cold-formed steel, which is typically channel section. Hence, this study aims to compare the buckling behavior of cold-formed steel channel sections, sigma sections, and built-up sigma sections. Experimental and numerical analyses were conducted to determine the buckling capacity of the cold-formed steel section subjected to axial compression. The load- deflection and failure modes are discussed in this study. Additionally, the strength-to-weight ratio of channel sections, sigma sections, and built-up sigma sections was compared. The built-up sigma section has superior performance relative to the single section. Furthermore, finding indicates that the sigma section surpasses the C-section.

**Keywords:** built-up section, channel section, cold-formed steel, sigma section, strength-to-weight ratio.

## INTRODUCTION

Light gauge steel sections are commonly used in a wide range of applications, from residential buildings to industrial facilities. Because it is a very thin element, understanding its buckling behavior when subjected to compression loads is crucial for ensuring its safety and reliability. There is no prior research has systematically evaluated and compared the strength-to-weight ratio of different cold-formed steel profiles. Existing studies primarily focus on the structural behavior, failure mechanisms, and optimization of individual sections, but a comprehensive investigation into their efficiency in terms of material utilization remains unexplored. This study aims to bridge this research gap by analysing the strength-to-weight ratio across various profiles, providing valuable insights for efficient design and material optimization in structural applications. Łukowicz et al. (2015) examined the classification of restraints in the optimization problem of a cold-formed profile, highlighting its complexity due to the need for extensive design and production considerations. This study identifies and categorizes restraints into three subsets: design assumptions, technological limitations, and standard conditions. Anbarasu and Murugapandian (2015) incorporated the behavior of cold-formed steel web-stiffened lipped channel columns experiencing distortional–global buckling mode interaction under axial compression. This study shows that global buckling was observed in the initial phase of testing, followed by distortional buckling in the later stages. Zhang and Young (2015) investigated cold-formed steel built-up columns with longitudinal stiffeners using a finite element analysis. Their study found that the modified design methods accurately predicted column strengths and improved resistance to buckling compared to conventional designs.

Urbańska-Galewska et al. (2016) investigated the effect of thin-walled cross-sectional shapes on the axial compression and bending moment resistance of cold-formed steel members. The study

analyzed four different cross-sectional geometries with a constant section area and thickness, considering three steel grades while accounting for local, distortional, and overall buckling effects. The findings highlight that compact sections exhibit better performance under compression, whereas slender and taller sections are more efficient under bending loads. Anbarasu and Venkatesan (2018) incorporated the behavior of cold-formed steel built-up I-section columns composed of four U-profiles under axial compression. A parametric study was conducted to examine the influence of the cross-sectional dimension ratios and lengths on the buckling behavior and ultimate strength. This study revealed that the incorporation of U-profiles, along with the presence of large lips in the top and bottom profiles, effectively mitigated the occurrence of distortional buckling failure. Fratamico et al. (2018) investigated the global buckling behavior of cold-formed steel sections connected by a self-drilling screw fastener at the web of the column. The results shows that the columns installing end fastener group (EFG) capacity increases 33% when compared to the columns without installing EFG. Zhang and Young (2018) incorporated various web stiffeners for closed built-up columns under axial compression. The results reveal that the moderated outward stiffener and deeper inward stiffener exhibit superior performance compared to the other sections.

Anbarasu (2019) investigated the behavior and strength of cold-formed steel built-up battened box columns composed of lipped angles under axial compression. Experimental tests on ten specimens, incorporating two different cross-sectional dimensions and five geometric lengths, were conducted under pinned conditions with warping restraints. Key influencing factors, including plate, member, chord slenderness, and batten plate slenderness, were analyzed. The author indicated a significant effect of chord slenderness on the compressive strength. Roy and Lim (2019) presented the behavior of a face-to-face built-up channel section cold-formed steel under axial compression. The authors studied the effects of different screw spacings on the different compositions of cold-formed steel columns. Hence the paper concluded that the vertical spacing increased by the two times between the fasteners, the axial strengths of short, intermediate and slender columns reduced by 5%, 12% and 22% respectively. Anbarasu (2019) conducted a numerical investigation of the structural response and ultimate resistance of cold-formed steel built-up columns composed of lipped sigma sections with pinned ends. The findings examined the influence of the member slenderness, height-to-width ratio, and trapezoidal stiffener depth on the ultimate resistance.

Anbarasu and Dar (2020) performed a numerical study on battened cold-formed steel box columns with four lipped angles. This validated model assessed the impact of sectional compactness, batten spacing, and column slenderness on buckling behavior, revealing limitations in current design rules related to unbraced chord slenderness and interconnector stiffness. Anbarasu and Dar (2020) conducted a numerical investigation of the axial capacity and nonlinear deformation response of pin-ended CFS built-up columns under monotonic axial loading. This study examined the effects of key parameters such as plate slenderness, unbraced chord slenderness, and global slenderness, on the ultimate compression resistance of these built-up columns. The author concluded that the inclusion of spacers effectively reduced the local buckling half-wavelength and enhanced the buckling resistance. Li and Young (2021) studied cold-formed steel built-up open section members under eccentric compressive loads. Specimens, 300–1500 mm long, made from G500 and G550 steel sheets, were tested for buckling behavior and the interaction between axial compression and bending. The tests revealed that the existing design codes generally underestimated the strength of these sections, as comparisons with predictions from various standards showed discrepancies in the axial load-moment interaction formulas. Mahar et al. (2021) investigated the compression behavior of back-to-back built-up cold-formed steel columns. The results indicated that the modified slenderness ratio (MSR) provided conservative predictions owing to the treatment of fastener spacing and slenderness ratio as separate factors. This study proposes a compound slenderness ratio (CSR) that captures their interaction, which, when used with the direct strength method (DSM), aligns well with experimental data and maintains reliability with AISI S100.

Aghoury et al. (2017) experimentally and numerically investigated the strength of a lipped sigma cold-formed steel column. These findings explain the varying flange width-to-thickness ratios, web return ratios, and overall slenderness. The results indicated local, distortional, and global buckling. The finite element capacities closely aligned with the predictions from the AISI and

DSM methods, confirming their accuracy. Aswathy and Kumar (2022) examined the interaction between flexural and torsional and flexural buckling modes in cold-formed steel unequal lipped-angle columns under axial compression. The results revealed that the lips of the section subjected to tensile stress were safer than those subjected to compression stresses. Rahnavard et al. (2023) examined composite action in cold-formed steel built-up battened columns with two sigma-shaped sections. Using finite element modelling, they determined that four rows of fasteners per batten panel and a minimum distance of 30 mm between the panels optimized the composite action. The analysis, comparing the results with EN1993-1-1 predictions, showed strong agreement, confirming the reliability of the EN1993-1-1 procedure with the AISI S100-16 slenderness ratio for CFS battened columns.

Mei et al. (2023) investigated the structural performance of G550 high-strength cold-formed steel-lipped channel columns under interactive buckling through experimental tests and numerical simulations. This finding revealed that although the effective width method (EWM) provided conservative results for columns with small to intermediate slenderness ratios, it was accurate for large slenderness ratios. He et al. (2024) explored the post-buckling behavior and design of cold-formed steel-lipped channel columns under local-distortional-global (L-D-G) interactions. The conclusion revealed that while the elastic critical buckling stresses were close, the D-G interaction significantly reduced the ultimate strength of the columns. Yılmaz et al. (2024) studied the buckling behavior of cold-formed sigma and lipped channel beam-columns under axial load and biaxial bending moments. The results revealed significant differences in the load-bearing capacity, energy absorption, and buckling modes of the two sections. The study showed that error rates decreased with longer sigma-section members and were lower for tensile stresses than for compressive stresses, with differences noted against the DSM based on loading and cross-sectional properties. Vijayamurugan et al. (2024) conducted the experimental and numerical investigations of the flexural strength of channel section cold-formed steel with variations in lip depth and web depth. This study concludes with the optimum size of the lip depth employed in the channel section. Additionally, the strength-to-weight ratio was analyzed to evaluate the overall performance of the sections.

This research focuses on the experimental and numerical investigation of the load-carrying capacity and buckling behavior of channel, sigma, and built-up sigma sections under compressive loading. This study examined the influence of varying section heights on structural performance. The findings highlight the load-carrying capacity of different cross-sections with varying lengths, the percentage increase in capacity, strength-to-weight ratio and a comparative analysis of the channel, sigma, and built-up sigma sections. Furthermore, the results demonstrate the superior performance of built-up sections over single sections, with sigma sections exhibiting greater strength than channel sections. Additionally, the sigma section exhibits a more favorable strength-to-weight ratio compared to both the channel and built-up sigma section.

## SPECIMEN DETAILS AND MATERIAL PROPERTIES

This study utilized the C-section, Sigma section, and Built-up Sigma section to examine the buckling capacity under compression. The precise measurements for all specimens are presented in Table 1. A pictorial representation of the symbols listed in Table 1 is shown

**Table 1.** Actual Dimensions of various section

| Specimen | Web depth (D) (mm) | Flange width (F) (mm) | Thickness (t) (mm) | Length (mm) | Web stiffener, mm | | |
|---|---|---|---|---|---|---|---|
| | | | | | W1 mm | W2 mm | W3 mm |
| C-160-40-2-555 | 160 | 40 | 2 | 555 | – | – | – |
| C-160-40-2-750 | 160 | 40 | 2 | 750 | – | – | – |
| S-160-40-2-555 | 160 | 40 | 2 | 555 | 40 | 20 | 40 |
| S-160-40-2-750 | 160 | 40 | 2 | 750 | 40 | 20 | 40 |
| BS-160-40-2-555 | 160 | 40 | 2 | 555 | 40 | 20 | 40 |
| BS-160-40-2-750 | 160 | 40 | 2 | 750 | 40 | 20 | 40 |

in Figure 1. The web depth, flange width, and thickness were 160, 40, and 2 mm, respectively. The heights of the columns were 750 mm and 555 mm for each C-section, sigma section, and built-up sigma section, respectively. This specimen designated was C-160-40-2-750. where C represents the channel section of the column. S denotes the sigma section of the column. BS denotes the built-up sigma section of the column. All dimensions are in millimeters. Figure 2 shows the nomenclature of the channel, sigma, and built-up sigma section.

Tensile coupon tests were conducted according to ASTM standards to determine the mechanical properties of the specimens. Three coupons were laser-cut longitudinally from identical steel sheets of 2.0 mm thickness before bending. Three coupons were tested under tension until failure, and the applied loads and strains were recorded. The average Young's modulus (E), yield stress (fy), ultimate tensile stress (fu), and elongation at failure (δ) values are presented in Table 2. The tensile coupon test set-up and stress-strain relationship for the thickness 2.0 mm as shown in Figure 3.

**a) Channel section** **b) Sigma section** **c) Back-to-back Sigma section**

**Figure 1.** Fabricated specimens

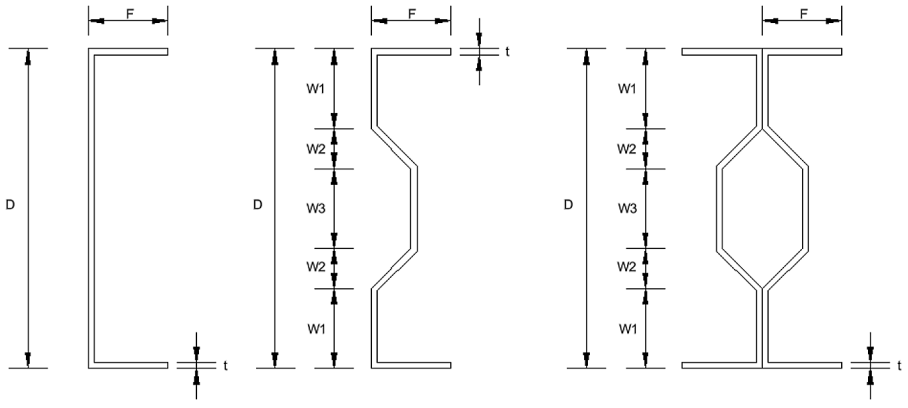


**Figure 2.** Cross section of channel section, sigma section and built-up sigma section

**Table 2.** Average material properties of coupon

| Specimen | Youngs modulus, MPa | Yield stress, MPa | Ultimate stress, MPa | Percentage elongation (%) |
|---|---|---|---|---|
| C-2 | 210341 | 255.66 | 350.69 | 37.3 |

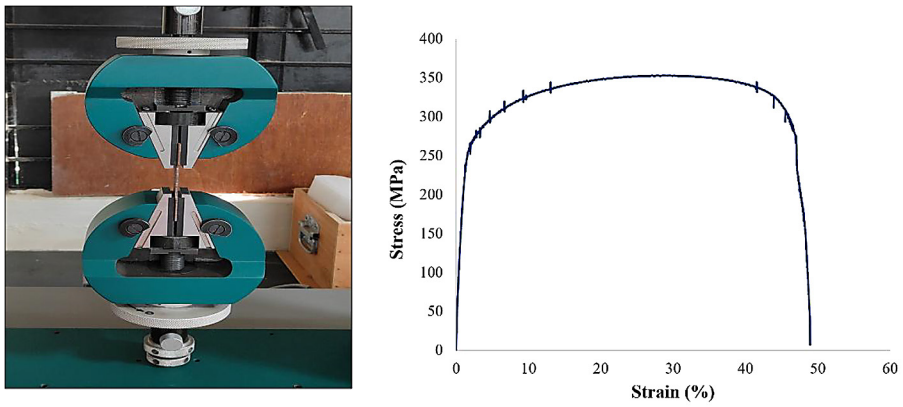


(a) Test set-up (b) Stress-Strain curve

**Figure 3.** Tensile coupon test set up and stress-strain curve

## EXPERIMENTAL STUDY

All specimens such as C-section, sigma section, and built-up sigma section were tested using a 1000 kN universal testing machine (UTM). The column was placed in the center line of the UTM to ensure that load passed axially, and the displacement is controlled to apply the load. The instrumentation contains an LVDT to measure the displacement, a load cell to measure the load, and a data logger to record the data. The loads were gradually applied until failure, and the load and deflection were continuously monitored and recorded using a data logger. The column was subjected to a loading condition in which one end was pinned, restricting translational movement while allowing rotational freedom, whereas the other end remained free, permitting both translational and rotational displacements under applied loading. The experimental setup is shown in Figure 4.

## FINITE ELEMENT ANALYSIS

Finite element analysis was conducted to determine the buckling capacity of the C-section, sigma section, and built-up sigma section columns. The S4R element, a quadrilateral four-node stress-displacement shell element with a large strain formulation, were employed in the

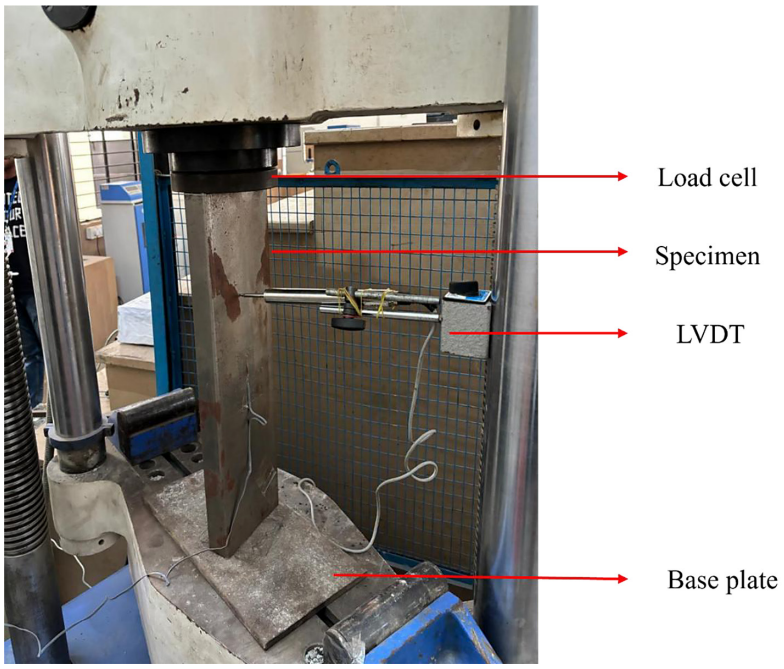


**Figure 4.** Experimental setup

analysis. The mesh size was selected based on a review of the literature and was finalized as 5 × 5 mm. The boundary conditions of the finite element models were validated, with one end of the column pinned and the other end free. The details of the modelling and analysis process are shown in Figure 5. The load and displacement were ascertained through the analysis. Figure 6 shows the finite element models of C-section, Sigma section, and built-up sigma section cold-formed steel. The details of the FE analysis process and the FE models are shown in Figure 5 and Figure 6 respectively.

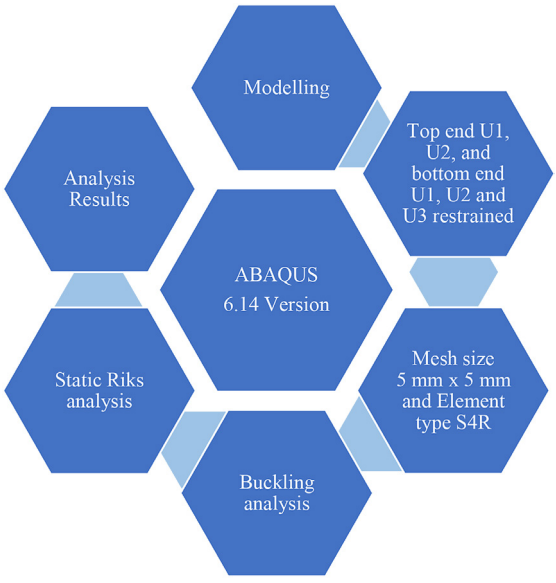


**Figure 5.** Details of FE analysis process

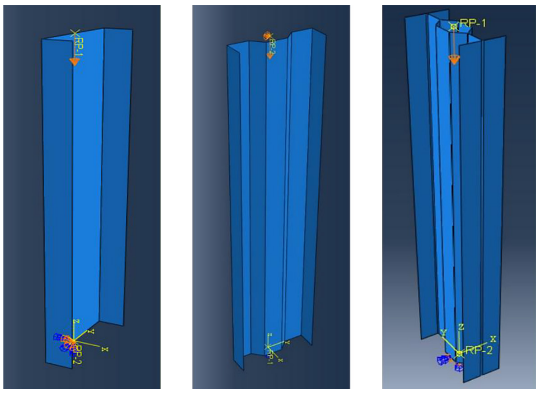


**Figure 6.** FE models

## RESULTS AND DISCUSSION

### Failure modes

The load was gradually increased until ultimate, and no failure was observed thereafter. Two types of failure modes were observed in the specimens: local and global buckling. The C-section behaved as flexible, unstable once load reaches near the ultimate load. After peak load lateral bulging (local buckling) was observed near the base of all the specimens. The sigma section was rigid and unstable when the load approached near the ultimate load. Initially lateral bulging was observed on the ends of the specimens, then failed by global buckling. The built-up sigma section also was rigid and stable when the load closer to the ultimate load, 555 mm height specimen crushed at the base. But, built-up sigma 750 mm height specimen, failed by combined local and global buckling. Both experimental and finite element analysis failure modes were similar. The experimental and numerical failure modes are shown in Figure 7 and Figure 8, respectively.

### Comparison of experimental and numerical study

The load-carrying capability and failure modes of the C-sections, sigma sections, and built-up sigma sections are listed in Table 3. The experimental results show that C-sections with lengths of 750 and 555 mm exhibited strengths of 48.32 kN and 52.50 kN, respectively. Correspondingly, the sigma section with dimensions of 750 mm and 555 mm exhibited values of 84.68 kN and 92.04 kN, respectively. The built-up sigma sections of 750 mm and 555 mm exhibited values of 170.94 kN and 199.32 kN, respectively. Similarly, the numerical results reveal the C-section of length 750 mm and 555 mm, exhibited strengths of 52.17 kN and 61.40 kN, respectively. Correspondingly, the sigma section with dimensions of 750 mm and 555 mm exhibited values of 93.08 kN and 99.11 kN, respectively. The built-up sigma sections of 750 mm and 555 mm exhibited values of 182.25 kN and 210.42 kN, respectively. Therefore, the numerical results show a similar match, which was validated using the experimental results. The built-up sigma section primarily enhanced the load-bearing capability as the column length decreases. The sigma section demonstrates superior performance compared to the C-section as the length increases, while the load-bearing capability decreased. The load – deflection behavior of the channel, sigma, and built-up sigma sections are depicted in Figure 9, 10 and 11, respectively.

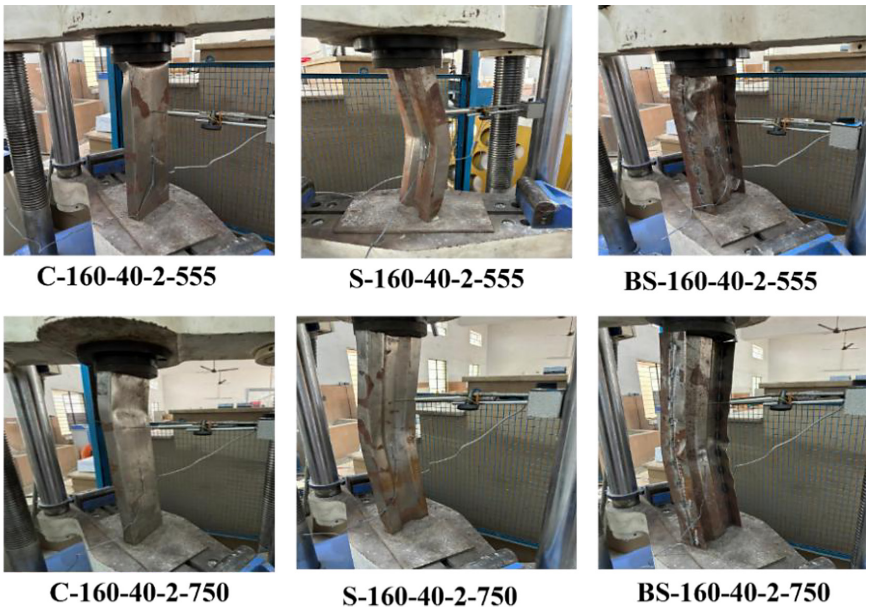


**Figure 7.** Failure mode of experimental study

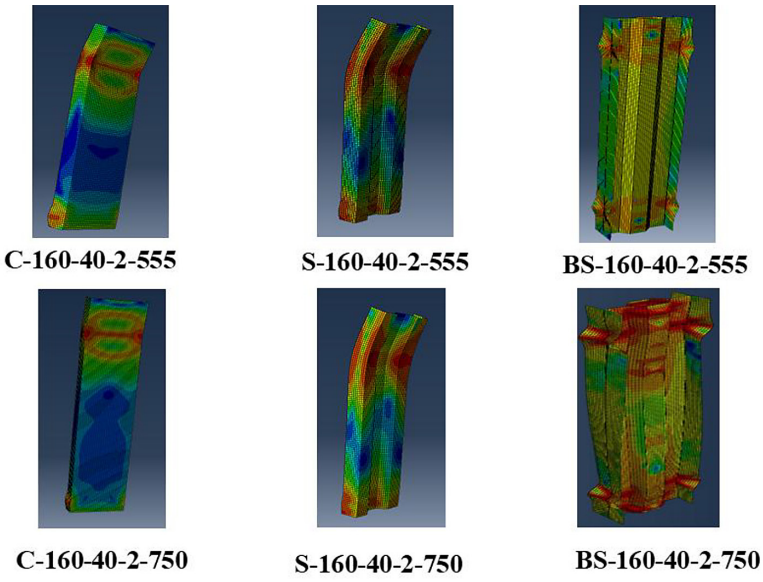


**Figure 8.** Failure mode of numerical study

**Table 3** Load carrying capacity and failure modes for all sections

| Specimen C-W-F-t-L | Load carrying capacity (kN) | | $P_{EXP}/P_{FEA}$ | Modes of failure |
|---|---|---|---|---|
| | $P_{EXP}$ | $P_{FEA}$ | | |
| C-160-40-2-555 | 51.50 | 61.40 | 0.84 | L |
| C-160-40-2-750 | 48.32 | 52.17 | 0.93 | L |
| S-160-40-2-555 | 92.04 | 99.11 | 0.93 | L+G |
| S-160-40-2-750 | 84.68 | 93.08 | 0.91 | L+G |
| BS-160-40-2-555 | 199.32 | 210.42 | 0.95 | L |
| BS-160-40-2-750 | 170.94 | 182.25 | 0.94 | L+G |
| Mean | | | 0.92 | |
| SD | | | 0.036 | |

**Note:** *L – local buckling, G – global buckling and SD – standard deviation.

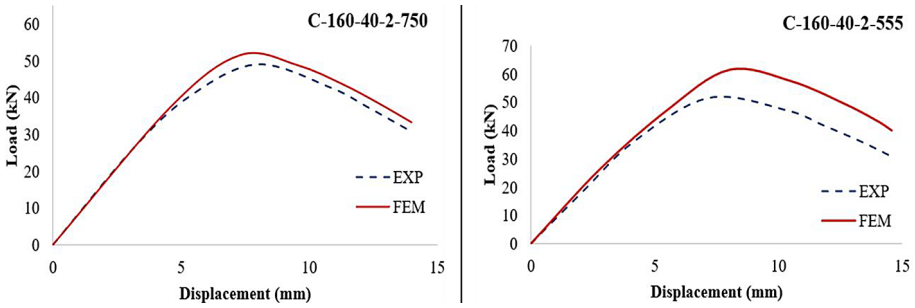


**Figure 9.** Load – displacement curve of channel section

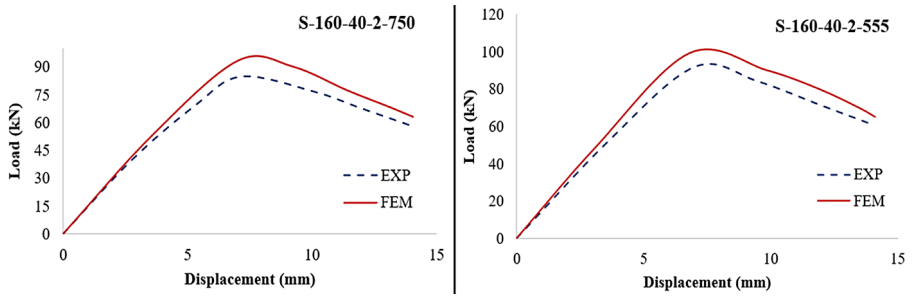


**Figure 10.** Load – displacement curve of sigma section

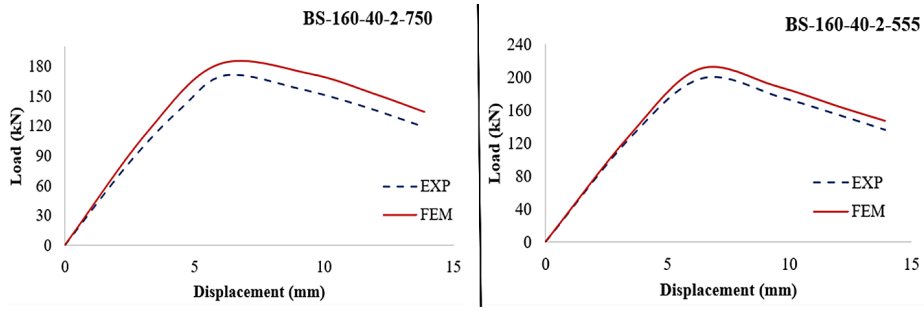


**Figure 11.** Load – displacement curve of built-up sigma section

## Influence of slenderness ratio on column

The slenderness ratio of a column is typically defined as the ratio of its effective length to its minimum radius of gyration. The key parameters influencing the slenderness include the unsupported length of the column, radius of gyration of the cross-section, and effective length factor. As the slenderness of the column increases, the failure mode gradually transitions from local to global buckling. This phenomenon was investigated by analyzing three distinct sections: channel, sigma, and built-up sigma sections, each designed with varying slenderness ratios. The sequence of the images illustrates the buckling behavior of a structural element under axial compression. Initially, the member remained stable; however, as the applied load increased, it began to exhibit elastic buckling. Upon reaching the critical buckling load, the element experienced significant inelastic deformations, leading to visible bending and localized plasticity. As the load continued to increase, the structure underwent progressive yielding and distortion, ultimately resulting in complete failure. This behavior emphasizes the interaction between local and distortional buckling, which is characteristic of thin-walled or highly slender structural elements subjected to compression.

## Percentage decrease in load carrying capacity

The percentage increase in load-carrying capacity was analyzed for three different section types: C-section, Sigma section, and built-up section across two lengths, 555 mm and 750 mm. The results, presented in Table 4, indicate

**Table 4.** Percentage increase in load carrying capacity

| Specimen | Load carrying capacity | Percentage of decrease in strength compared to 555 mm specimen (%) |
|---|---|---|
| | $P_{EXP}$ (kN) | |
| C-160-40-2-555 | 51.50 | – |
| S-160-40-2-555 | 92.04 | – |
| BS-160-40-2-555 | 199.32 | – |
| C-160-40-2-750 | 48.32 | 6.17 |
| S-160-40-2-750 | 84.68 | 8.00 |
| BS-160-40-2-750 | 170.94 | 14.24 |

notable variations in the percentage increase in the load-carrying capacity based on the length. The strengths of the 750 mm section for the C-section, sigma section, and built-up sigma section decreased by 6.17%, 8.00%, and 14.24%, respectively, compared to the 555 mm. The Sigma section demonstrated a significant improvement in the load-carrying capacity compared to the C-section. Furthermore, the built-up sigma section exhibited better performance than single sections.

## Comparison of C-section, sigma section and built-up sigma section

A comparison of cold-formed steel columns with C-section, sigma section, and built-up sigma section profiles revealed distinct differences in structural performance. The C-section exhibited the lowest load-bearing capacity owing to its simpler geometry and reduced stiffness, making it more prone to buckling. The sigma section, with a more complex geometry, exhibited higher strength and greater resistance to buckling than the C-section. However, the built-up sigma section outperformed both, offering the highest load-bearing capacity owing to its composite configuration, which enhanced the stiffness and stability. This indicates that built-up sections are ideal for heavy-load applications that require superior strength, as shown in Figure 12.

## Strength-to-weight ratio

The strength-to-weight ratio is a critical parameter in for assessing the performance of cold-formed steel sections. Strength is defined as the ratio of the ultimate load to the cross-sectional area. For a column with a height of 555 mm, the calculated strengths for the channel, sigma, and built-up sigma section were 109.15 MPa, 189.51 MPa, and 205.21 MPa, respectively. Similarly, for a column with a height of 750 mm, the strengths were 102.41 MPa, 174.36 MPa, and 175.99 MPa, respectively. While the ultimate load capacity did not show significant differences between the sigma and built-up sigma sections, the strength-to-weight ratio analysis indicated that the sigma section outperformed the built-up sigma section (Table 5). This superior performance is attributed to the smaller cross-sectional area of the sigma

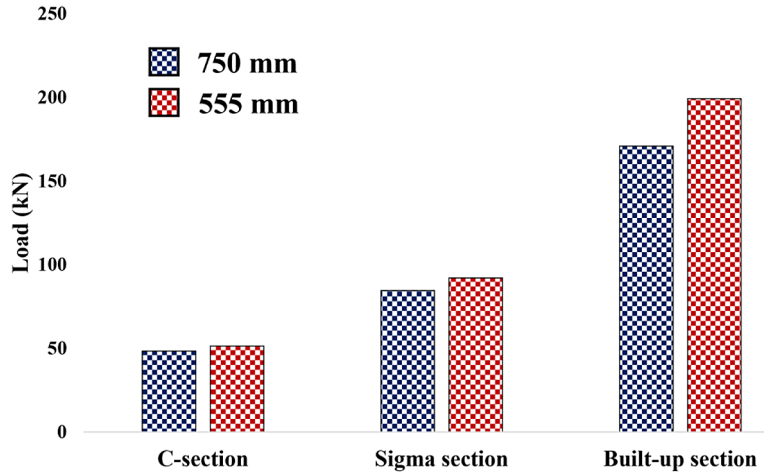


**Figure 12.** Comparison of different section with various length

**Table 5.** Strength-to-weight ratio

| Specimen | Strength | Weight | Ratio |
|---|---|---|---|
| | Kg/mm² | kg | |
| C-160-40-2-555 | 11.126 | 2.06 | 5.41 |
| S-160-40-2-555 | 19.319 | 2.12 | 9.13 |
| BS-160-40-2-555 | 20.918 | 4.23 | 4.94 |
| C-160-40-2-750 | 10.439 | 2.78 | 3.76 |
| S-160-40-2-750 | 17.774 | 2.86 | 6.21 |
| BS-160-40-2-750 | 17.940 | 5.72 | 3.14 |

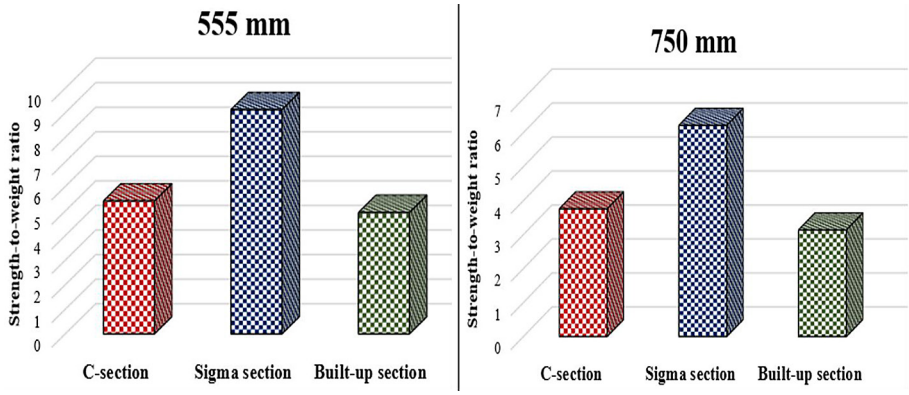


**Figure 13.** Strength-to-weight ratio of column height 555 mm and 750 mm

section, which effectively doubles its efficiency in terms of the weight. The strength-to-weight ratios of the column heights of 555 and 750 mm are shown in Figure 13.

## CONCLUSIONS

This study presents an experimental and numerical investigation of cold-formed steel C-section, sigma section, and built-up sigma section profiles under compression by varying the height. The key findings of this analysis are as follows:

1. The strength-to-weight ratio of the sigma section was higher than of the built-up sigma section and C-section.
2. The column height significantly influences the structural performance. The shorter length column carries more load than the longer length column.
3. Percentage of increase in strength of sigma section is nearly 75 % compared to C section and percentage of increase in strength of built-up sigma section is nearly 250 % compared to C section.
4. The built-up sigma section exhibited the highest strength, outperforming both the C-section and sigma section. Additionally, the sigma section displayed a superior load-bearing capacity compared with the C-section.

The study highlights the superior strength and efficiency of sigma and built-up sigma sections, making them suitable for lightweight and high-performance structural applications. The built-up sigma section, with its enhanced load-bearing capacity, is ideal for modular and prefabricated constructions. Additionally, the influence of column height on strength emphasizes the need for an optimal design for cold-formed steel structures.

Future research can explore the behavior of sigma and built-up sigma sections under combined bending and compression by varying the length.

## REFERENCES

1. Łukowicz A, Urbańska-Galewska E, Deniziak P, Gordziej-Zagórowska M. Classification of restraints in the optimization problem of a cold-formed profile. Advances in Science and Technology – Research Journal. 2015 Jan 1;9(28):61–7.
2. Anbarasu M, Murugapandian G. Experimental study on cold-formed steel web stiffened lipped channel columns undergoing distortional–global

interaction. Materials and Structures. 2015 Mar 8;49(4):1433–42.

3. Zhang JH, Young B. Numerical investigation and design of cold-formed steel built-up open section columns with longitudinal stiffeners. Thin-Walled Structures. 2015 Apr; 89:178–91.
4. Urbańska-Galewska E, Deniziak P, Gordziej-Zagórowska M, Łukowicz A. Thin-walled cross section shape influence on steel member resistance. Advances in Science and Technology Research Journal. 2016;10(29):41–5.
5. Anbarasu M, Venkatesan M. Behaviour of cold-formed steel built-up I-section columns composed of four U-profiles. Advances in Structural Engineering. 2018 Sep 7;22(3):613–25.
6. Fratamico DC, Torabian S, Zhao X, Rasmussen KJR, Schafer BW. Experiments on the global buckling and collapse of built-up cold-formed steel columns. Journal of Constructional Steel Research. 2018 May; 144:65–80.
7. Zhang JH, Young B. Finite element analysis and design of cold-formed steel built-up closed section columns with web stiffeners. Thin-Walled Structures. 2018 Oct; 131:223–37.
8. Anbarasu M. Behaviour of cold-formed steel built-up battened columns composed of four lipped angles: Tests and numerical validation. Advances in Structural Engineering. 2019 Jul 26;23(1):51–64.
9. Roy K, Lim JBP. Numerical investigation into the buckling behaviour of face-to-face built-up cold-formed stainless steel channel sections under axial compression. Structures. 2019 Aug; 20:42–73.
10. Anbarasu M. Numerical investigation on behaviour and design of cold-formed steel built-up column composed of lipped sigma channels. Advances in Structural Engineering. 2019 Feb 3;22(8):1817–29.
11. Anbarasu M, Adil Dar M. Axial capacity of CFS built-up columns comprising of lipped channels with spacers: Nonlinear response and design. Engineering Structures. 2020 Jun 1; 213:110559–9.
12. Anbarasu M, Dar MA. Improved design procedure for battened cold-formed steel built-up columns composed of lipped angles. Journal of Constructional Steel Research. 2020 Jan; 164:105781.
13. Li QY, Young B. Tests of cold-formed steel built-up open section members under eccentric compressive load. Journal of Constructional Steel Research. 2021 Sep; 184:106775.
14. Mahar AM, Jayachandran SA, Mahendran M. Global buckling strength of discretely fastened back-to-back built-up cold-formed steel columns. Journal of Constructional Steel Research. 2021 Dec; 187:106998.
15. El Aghoury MA, Hanna MT, Amoush EA. Experimental and theoretical investigation of cold-formed single lipped sigma columns. Thin-Walled Structures. 2016 Dec 27; 111:80–92.
16. Kalam Aswathy KC, Kumar MVA. Interaction behavior of fixed ended cold-formed steel unequal lipped angle columns. Thin-Walled Structures. 2024 May 27; 202:112056–6.
17. Rahnavard R, Razavi M, Fanaie N, Craveiro HD. Evaluation of the composite action of cold-formed steel built-up battened columns composed of two sigma-shaped sections. Thin-walled structures. 2023 Feb 1; 183:110390–0.
18. Mei Y, Cui Y, Ma C, Sun Y, Su A. Tests, numerical simulations and design of G550 high strength cold-formed steel lipped channel section columns failing by interactive buckling. Thin-walled structures. 2023 Nov 1;192:111172–2.
19. He Z, Zhang Y, Zhou X, Zou B, Zhang Z. Post-buckling behavior and DSM design of cold-formed steel lipped channel columns experiencing local-distortional-global interaction. Structures. 2024 Sep; 67:106945.
20. Yılmaz Y, Öztürk F, Buckling DS. Behavior of cold-formed steel sigma and lipped channel section beam-columns: Experimental and numerical investigation. Journal of Constructional Steel Research. 2024 Mar 1; 214:108456–6.
21. Vijayamurugan N, Prabaharan V, Akhas P Kumar. Effect of lip depth on the flexural capacity of cold-formed steel section. International Journal of Steel Structures. 2024 Jul 8;24(4):849–61.